Int. J. Adv. Eng. Pure Sci. 2024, 36(3): <278-289>
DOI: 10.7240/jeps.1507109

RESEARCH ARTICLE / ARAŞTIRMA MAKALESİ

Effects of Spreading Parameters on Powder Bed Quality

Muhammet Furkan ÇOŞKUN [1], **Recep ÖNLER** [1]

[1]*Gebze Technical University (GTU), Department of Mechanical Engineering, 41400, Kocaeli, Türkiye*

Abstract

Powder bed-based additive manufacturing processes such as laser powder bed fusion, binder jetting, and electron beam melting are commonly utilized in various critical areas such as medical, aviation, and energy. Common to all these operations, the powders are first spread onto the build platform in a layer-by-layer fashion and selectively fused or bound with a suitable method. The quality of the process depends on several parameters, including how the powders are spread onto the build platform. The powder spreading operation, which involves spreading powders on a powder bed with a roller or spreader, is an important step in these operations and can affect various process outputs. In this study, powder spreading is numerically investigated using the discrete element method to determine the effects of layer thickness, rotation, and translation velocities, selected as parameters with a powder spreader roller. To account for the relationship between powder spreading parameters and the powder volume packing fraction, as well as the interactions between particles themselves and between the particles and the build plate, the Hertz-Mindlin contact model, including normal tangential forces, as well as the Johnson-Kendall-Roberts (JKR) contact model, including the effects of surface energy, were added to the numerical model. A Design of Experiment combined with analysis of variance (ANOVA) was utilized to gain a broader understanding of the relationship between process parameters, green density, and dynamic angle of repose.

Keywords: Additive Manufacturing, Powder Spreading, Discrete Element Method, ANOVA

Öz

Lazerle toz yatağında füzyon, bağlayıcı püskürtme ve elektron ışını ile ergitme gibi toz yatağı tabanlı yöntemler, tıbbi, havacılık ve enerji gibi çeşitli kritik alanlarda yaygın olarak kullanılmaktadır. Bu işlemlerin hepsinde ortak olarak, tozlar önce katman üretim platformuna yayılır ve uygun bir yöntemle seçici olarak ergitilir veya bağlanır. Sürecin kalitesi, tozların üretim platformuna nasıl yayıldığı da dahil olmak üzere birçok süreç parametresine bağlıdır. Bir merdaneyle veya yayıcı ile tozların toz yatağına serilmesi işlemi olan toz yayma operasyonu, bu işlemlerde önemli bir adımdır ve yoğunluk, yüzey pürüzlülüğü gibi çeşitli süreç çıktıları üzerinde etkili olabilir. Bu çalışmada, toz yayma, katman kalınlığı, dönüş ve geçiş hızlarının parametre olarak seçildiği bir toz yayıcı silindiri ile, ayrık elemanlar yöntemi kullanılarak sayısal olarak incelenmiştir. Toz yayma parametreleri ile toz hacim paketleme oranı arasındaki ilişki, partiküllerin kendileri arasında ve partikül ile üretim plakası arasındaki etkileşimleri dikkate almak için normal ve teğetsel kuvvetleri içeren Hertz-Mindlin temas modelinin yanında yüzey enerjisinin etkilerini içeren Johnson-Kendall-Roberts (JKR) temas modeli sayısal modele eklenmiştir. Deney Tasarımı ve varyans analizi (ANOVA) ile birleştirilmiş olarak, süreç parametreleri ile yoğunluk ve dinamik yığın açısı arasındaki ilişkiyi daha geniş bir anlayış kazanmak için kullanılmıştır.

Anahtar Kelimeler: Eklemeli İmalat, Toz Serpme, Ayrık Elemanlar Yöntemi, ANOVA

I. INTRODUCTION

Additive manufacturing has been proven to be an effective and versatile approach to produce intricate geometries from a variety of materials [1]. Its geometric capabilities are beyond comparison with traditional techniques. Among additive manufacturing processes, powder bed-based processes such as laser/electron beam powder bed fusion and binder jetting have found numerous critical applications in many industries [2]. In these processes, powder fed to the system with either a piston-based or hopper-based system is spread onto the build platform using a spreader. The powder is then selectively melted or bound together by a suitable means depending on the manufacturing type used. In general, the spreading operation is employed using either a roller, knife, or brush. Depending on the spreading conditions, final part quality may be affected. Thus, it is imperative to understand the effects of powder spreading conditions on powder bed quality [3].

Corresponding Author: RECEP ÖNLER, **Tel:** +90 262 605 27 79, **E-mail:** ronler@gtu.edu.tr

Submitted: 29.06.2024, **Revised:** 01.08.2024, **Accepted:** 18.08.2024

Although the final geometry is obtained after melting the powder in fusion-based powder bed processes or after sintering in binder jetting operations, it has been shown that the powder bed quality can affect the final part [4]. The powder bed quality also has a detrimental effect on energy absorption in powder bed fusion [5]. In binder jetting, it can significantly affect the powder-binder interaction, sintering, and infiltration behavior [6]. The quality of the powder layer in the powder spreading process is influenced by the geometry, motion, and material properties of the spreading tool. Additionally, the powder feedstock and its characteristics play a significant role, impacting both the powder layer quality and, consequently, the final product's properties and overall quality.

Several studies have examined various aspects of powder spreading in additive manufacturing using both experimental and numerical methodologies. For instance, Onler et al. explored the impact of powder spreading parameters, alongside other process variables, in binder jet additive manufacturing. They found that factors such as layer thickness, roller rotation direction, and roller transverse velocity significantly affect both green part densities and quality [7]. Gilebart et al. highlighted the importance of both assembling procedures and contact laws in determining the properties of cohesive powders. Through detailed simulations, they provided insights that can be used to better control and predict the behavior of these materials in practical applications [8]. Maximenko et al. investigated the influence of powder spreading parameters on part distortion during binder jetting using the discrete element method. Their findings suggested that the distortion of previously deposited layers depends on factors such as the amount of powder removed during spreading, the thicknesses of the deposited layers, and the dimensions of the manufactured components. Through modeling and simulation, they provided insights and guidelines for optimizing the powder spreading process, contributing to better control over the final dimensions and quality of binder-jetted parts [9]. Zhang et al. integrated the discrete element method with neural networks to develop a powder spreading process map. Their study highlighted the dominant role of the rotational speed of the roller in determining the surface roughness of the spread layer [10]. Additionally, Miyanaji et al. demonstrated the importance of powder characteristics in the binder jetting process, showing that particle size, shape, distribution, and flowability significantly affect the quality and properties of the fabricated parts. By optimizing these powder characteristics, manufacturers can achieve better control over the binder jetting process and produce high-quality parts. They also presented a comprehensive study on optimizing the binder jetting process for printing green parts, highlighting the importance of binder saturation, layer thickness, and powder characteristics. By fine-tuning these parameters, manufacturers can achieve high-quality green parts, paving the way for improved final products after sintering [11,12].

The discrete element method (DEM), pioneered by Cundall and Strack, has been widely utilized for particle analysis and simulations across various systems. Given the difficulties and expenses associated with experimentally investigating powder spreading, DEM offers a cost-effective and powerful platform for understanding powder spreading in additive manufacturing. For instance, Parteli and Paschel developed a numerical workbench to analyze the effects of surface roughness due to these parameters. They demonstrated the utility of particle-based simulations in studying and optimizing the powder application process in additive manufacturing. By analyzing the effects of particle properties and spreading mechanisms, their study provides valuable insights for achieving better control over powder layer quality, ultimately enhancing the performance and reliability of additive manufacturing processes [13]. Meanwhile, Mindt et al. monitored the load during the spreading process of titanium alloy powder. They highlighted the often-overlooked importance of powder bed layer characteristics as a primary input in additive manufacturing. By demonstrating how these characteristics influence final part quality, their study calls for improved control and optimization of the powder bed layer to achieve better outcomes in AM processes [14]. Haeri et al. investigated the effects of speed parameters on coating and plate displacement, revealing that cylindrical spreaders are superior to blade types in terms of powder packing density. Their study demonstrates the potential of using DEM simulations to optimize blade-type spreaders for powder bed preparation in additive manufacturing. By identifying the optimal blade design and operational parameters, they provide valuable insights for improving the uniformity and quality of powder layers, ultimately enhancing AM process performance [15]. Chen et al. and Meier et al. employed DEM-based numerical models to investigate particle dynamics and the powder recoating process, respectively, validating their findings with experiments [16]. Nan et al. studied friction-induced jamming in powders experimentally and incorporated these findings into simulations [17]. Fouda et al. analyzed the effects of particle material and spreader type on packing density, emphasizing process parameters and system mechanisms. Their study examines the behavior of powder particles during the spreading process and identifies factors influencing the uniformity and density of the powder layer. Key findings highlight the importance of particle size, shape, and cohesion in achieving a consistent powder bed, which is crucial for the quality of the final manufactured parts. Their results provide insights for optimizing the spreading process to improve additive manufacturing outcomes [18]. Han et al. developed a systematic approach to determine the optimal layer

thickness considering packing density, correlating it with microstructure and tensile strength. Their study investigates how parameters such as particle size distribution and spreading speed affect the thickness and uniformity of the powder layer. The findings indicate that optimal control of these parameters can lead to more consistent layer thickness, which is essential for high-quality additive manufacturing parts [19]. Phua et al. calibrated particle properties using DEM-based models, matching experimental measurements. Their results demonstrate how surface roughness and features impact the uniformity of new powder layers [20]. Gurnon et al. proposed a multi-layer DEM model, contrasting with single-layer studies, and validated it experimentally. Their findings emphasize that precise control of spreading dynamics is essential for achieving high-quality powder layers, which in turn influence the final part properties [21]. Chen et al. introduced a counterclockwise rotating roller in DEM-based analysis, offering new insights into physical mechanisms [22], while Valerio et al. elucidated spreading operations using a numerical DEM model [23].

As summarized above, powder spreading plays a crucial role in powder bed-based additive manufacturing processes. Although various aspects of powder spreading have been comprehensively investigated in the literature, discrete element-based approaches can be further useful for improving powder spreading without incurring experimental costs. Hence, this study focuses on the statistical analysis of spreading parameters on powder bed quality. To achieve this, a full factorial design of experiment-based DEM simulations has been carried out. Analysis of Variance (ANOVA)-based statistical investigations were performed to identify the relationship between spreading parameters and both powder density and the dynamic angle of repose.

The optimization of powder spreading in powder bed-based additive manufacturing processes is crucial for ensuring high-quality output in critical applications such as medical implants, aerospace components, and energy systems. Despite the significant role of powder spreading, there is limited understanding of how specific parameters like layer thickness, roller rotation and translation velocities impact the final product's quality. This study addresses this gap by employing the discrete element method (DEM) to numerically investigate these effects, incorporating advanced contact models to capture the intricate interactions between particles and the build platform using a design of experiment, ANOVA and response surface method (RSM) based statistical approaches. This study approach provides deeper insights into the mechanics of powder spreading, enabling better control and optimization of additive manufacturing processes, ultimately leading to enhanced product performance and reliability.

II. METHOD

2.1. Discrete Element Method

The Discrete Element Method (DEM) is a powerful numerical technique employed to simulate systems composed of numerous discrete particles [18]. A typical DEM simulation begins with the initialization phase, where particles are spatially oriented and assigned initial velocities. This is followed by the explicit time-stepping phase, where forces acting on each particle are computed based on initial conditions, physical laws, and contact models. Nearest neighbor sorting is periodically conducted during this phase to reduce computational complexity by limiting the number of potential contact pairs. Forces considered in macroscopic simulations include friction, contact plasticity or recoil, gravity, and various attractive potentials such as cohesion, adhesion, liquid bridging, and electrostatic attraction.

2.2. Governing Equation

A ‘super-spherical approach’ was used for the particle type because powders exhibit very dense particle flow and require effective layering during the spreading process [22,24]. In this layering process, the motion of powder particles is governed by Newton's second law of motion, which describes the individual translational and rotational motion of particles. As depicted in Figure 1, the equations governing the motion of each particle in the system at time '*t*', arising from interactions with other particles *'j'* present in the system or with other components, can be expressed as follows:

$$m_i \frac{du_i}{dt} = G_i + \sum_j \left(F_{ij}^n + F_{ij}^\tau\right) \quad \textbf{(1)}$$

$$I_i \frac{dw_i}{dt} = \sum_j \left(T_{f,ij} + T_{r,ij}\right) \quad \textbf{(2)}$$

Where u_i, I_i, m_i and ω_i are, respectively, translational velocity, moment of inertia, the mass, and rotational velocity of particle *i*; F_{ij}^n and F_{ij}^τ are, respectively, the normal and tangential interaction forces between particle *i* and *j*. G_i is the gravitational force of particle *i*. The normal and tangential forces inherent in the system can be derived directly from the contact and damping force formulas, i.e., $F_{ij}^n = F_{c,ij}^\eta + F_{d,ij}^n$ and $F_{ij}^\tau = F_{c,ij}^\tau + F_{d,ij}^\tau$. Then, the model proposed by Tsuji et al [25], this model is also based on the Hert-Mindlin contact force model, simplified for ease of use, which makes an acceptable accuracy demonstrate of the particle dynamic behavior during the particle contacts [26], is applied to calculate the damping forces ($F_{d,ij}^n$ and $F_{d,ij}^\tau$) and tangential contact forces $F_{c,ij}^\tau$ as a result of the deformation of the particles. $T_{f,ij}$ is the torque which is formed by the contact forces driving the other particle which cause particle *i* to rotate, and $T_{r,ij}$ is the rolling friction torque that opposes to the rotation of particle *i*.

Van der Waals forces begin to dominate when the diameters of the particles in the system are smaller than 100 microns. Consequently, calculating cohesion forces between particles becomes necessary. The JKR contact model addresses this requirement. The JKR contact model is essentially an extension of the Hertz-Mindlin contact model, designed to calculate contact forces acting on elastic and adhesive particles. Equations 3 and 4 are used to determine the contact radius and pull-off force, respectively.

$$a = \frac{a^2}{R^*} - 2\left(\frac{\pi\gamma a}{E^*}\right)^{1/2} \quad \textbf{(3)}$$

$$F_n = \frac{4E^*a^3}{3R^*} - 4(\pi\gamma E^* a^3)^{1/2} \quad \textbf{(4)}$$

Where a, γ and E are circular are of radius, surface energy and young modulus, respectively.

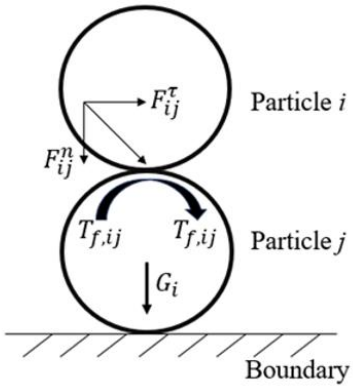

Figure 1. Illustration of force and torque for two interacting super-spherical particles

2.3. Material

To simulate particle dynamic behaviors and their fundamentals using DEM, the material properties and conditions must be accurately described and input into the program as parameters and boundaries. Although some of these parameters are challenging to measure [27], they are often sourced directly from the literature [18,28].

In this study, Ti6Al4V (Titanium Alloy), which is widely used in additive manufacturing, is employed to provide a common basis for comparison. The physical and mechanical properties of the particulate material required for the simulations are listed in Table 1. These properties are characterized by their specific applications and have been defined in previous studies. Commercial steel is chosen as the material for the build plate [29].

Table 1. Properties and input parameters of Ti6Al4V (Titanium Alloy) material [18]

Properties	Clearance
Particle Material Density (kg/m^3)	4300
Walls Material Density (kg/m^3)	8500
Particle Shear Modulus (MPa)	1
Particle Poisson Ratio	0.3
Wall Shear Modulus (MPa)	1
Wall Poisson Ratio	0.3
Particle-Particle Coefficient of Restitution	0.5
Particle-Wall Coefficient of Restitution	0.5
Particle-Particle Coefficient of Sliding Friction	0.5
Particle-Wall Coefficient of Sliding Friction	0.5
Particle-Particle Coefficient of Rolling Friction	0.01
Particle-Wall Coefficient of Rolling Friction	0.1

2.4. Particle Size Distribution and Layer Thickness

Particle size distribution is a critical parameter for the spreading operation and has both positive and negative effects on packing fraction. Various particle distribution methods are used in the literature, such as random, half-normal, log-normal, and linear-normal distributions. For a more precise simulation, gas-atomized Ti-6Al-4V powders were considered. Particle size distributions were measured using a particle size analyzer (Mastersizer-2000, Malvern), and particle morphology was assessed using scanning electron microscopy (XL30 SFEG, Philips). As shown in Figure 2, the particle diameter distribution is approximately 50 microns, with particles close to this diameter occupying most of the total volume. Among the investigated particle distributions, the log-normal size distribution was found to be more representative of the actual conditions than the others. Therefore, the particle diameter distribution was chosen based on the log-normal size distribution [30].

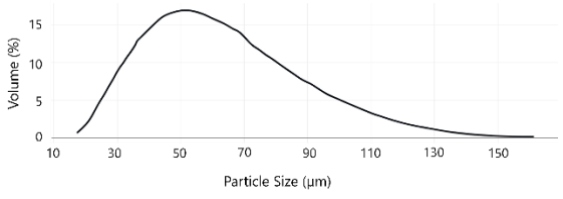

Figure 2. A sample particle size distribution of Ti-6Al-4V powders considered in the simulation

In this study, the particle diameter was set to 50 microns, and the log-normal size distribution was defined with a standard deviation of 0.05 and a mean of zero for all materials. As shown in the scanning electron microscopy images in Figure 3, the particles are predominantly spherical, with a small number of

satellite-shaped particles. Therefore, super-spherical-shaped particles were modeled, consistent with approaches used in the literature [8].

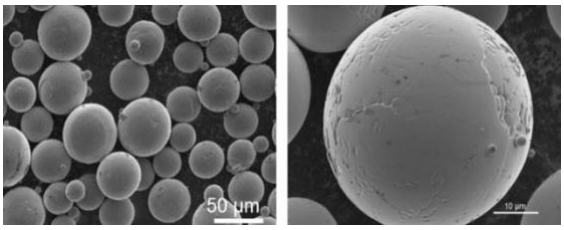

Figure 3. Scanning Electron Microscopy images of Ti-6Al-4V particles considered in the study

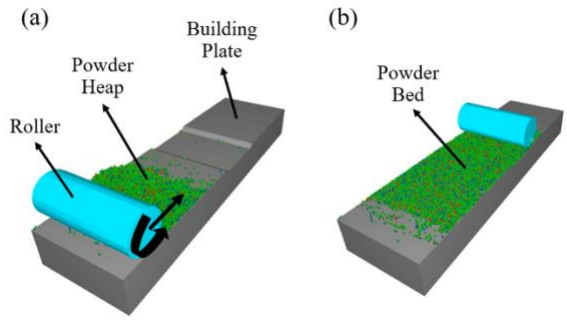

Figure 4. DEM simulation set-up showing roller, feedstock and building plate (a) before, and (b) after the spreading operation for one layer

2.5. Simulation Setup

A powder spreading system, featuring a spreader and a build plate, is commonly used in production methods such as Selective Laser Melting (SLM), Binder Jetting (BJ), and Selective Electron Beam Melting (SEBM). This system, modeled as shown in Figure 4, consists of three main components: the roller, the powder heap, and the build plate, which defines the layer geometry by providing the desired depth. As illustrated in Figure 4(a), powders are produced at a rate of ten thousand units per second using a virtual plate positioned appropriately within the system. These powders are deposited in front of the roller under the influence of gravity, forming a heap. After the heap is formed by the virtual plate, the roller rotates at a specific angular velocity and moves forward at a set translational speed to fill the gap created by the layer thickness on the build plate, thereby forming the powder bed, as shown in Figure 4(b). Another critical physical parameter is the vertical gap between the roller and the build plate, which directly impacts the system. This gap affects the packing density of the deposited powder and its surface roughness, which corresponds to the vertical resolution of the 3D printed component. In the simulations performed for this study, the gap was maintained at a constant 50 microns, a standard value used in typical electron beam melting (EBM) machines [31,32]. This standardization ensures consistency and allows meaningful comparisons between simulation results and real-world manufacturing processes.

The discrete element method (DEM) is a numerical technique well-suited for predicting the motion of individual powder particles and their dynamics during the powder spreading process. Due to these capabilities, DEM has been used extensively in simulations. In this paper, varying simulations were conducted using the DEM software EDEM® provided by Altair. To achieve more accurate results, the Hertz-Mindlin and Johnson-Kendall-Roberts (JKR) contact models were employed to determine interactions between particles and between particles and walls.

2.6. Simulation Parameters

In this study, we employed a full factorial design of experiments approach, incorporating layer thickness, rotational speed, and translational speed as key factors. The layer thickness values chosen were 100, 120, 130, and 140 µm. The roller rotational velocities were set at 150, 200, and 250 rpm, while the roller translational velocities were set at 10, 20, and 30 mm/sec. These parameter choices were informed by previous studies [18,23,33]. With 4 levels of layer thickness and 3 levels each of rotational and translational velocities, a total of 36 simulations were conducted to thoroughly explore the parameter space and analyze their effects on the system.

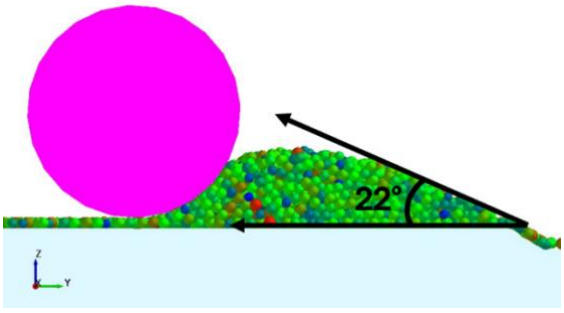

Figure 5. Virtual measurement of dynamic angle of repose

2.6.1. Dynamic angle of repose and packing fraction measurements

The dynamic angle of repose for different rotational and translational velocities at each layer thickness was measured by capturing screenshots at various time intervals, ensuring that the rollers were in identical positions. To pinpoint the precise moment for determining the dynamic angle of repose, all time steps of the simulation were carefully reviewed. The specific moment when the powders first filled the space designated for the layer thickness, as shown in Figure 5, was identified as the time to reach the steady state, as suggested by [34]. This approach enabled a precise assessment and analysis of the dynamic angle of repose under the varying experimental conditions.

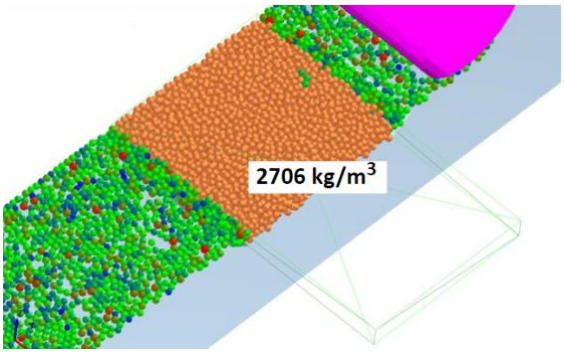

Figure 6. Virtual box employed for measurement of volume packing fraction

In this study, the volume packing fraction defined as the percentage of the total volume of powders within a given unit volume was measured for different rotational and translational velocities at each layer thickness. This measurement was conducted using a virtual box within the EDEM simulation environment, as shown in Figure 6. The density sensor box was designed to fully encompass the layer thickness to ensure accurate density measurements. The positioning of the layer thickness for density determination was carefully aligned to cover the entire layer thickness, in accordance with established practices [16,35]. This approach enabled a precise and thorough assessment of the volume packing fraction under various experimental conditions.

Figure 7. Virtual box employed for measurement of volume packing fraction

2.6.2. Analysis of Variance

To assess the impact of the examined parameters, we utilized a commonly employed statistical method known as Analysis of Variance (ANOVA). ANOVA is frequently used to ascertain if there are any statistically significant distinctions among the means of various groups. Statistical comparisons were conducted using a two-tailed Student's t-test, with a significance threshold of $p < 0.05$. Additionally, to better interpret the ANOVA outcomes beyond mere statistical significance, we calculated the relative contributions of spreading parameters and their interactions [36]. The ANOVA results pertaining to parameters with substantial contributions were subsequently tabulated and graphically represented.

III. RESULTS

3.1 Dynamic Angle of Repose

Figure 7 illustrates the main effects of how spreading parameters influence the dynamic angle of repose, which consistently ranges from 23° to 32° under various conditions. In this figure, the y axis shows the mean of the simulations results generated using the identical individual simulation parameter. Fon instance, the first point corresponding to 100 µm layer thickness considers all the rotational and transitional velocity combinations with 100 µmm layer thickness. The angle of repose was found to increase linearly with layer thickness. In contrast, rotational and translational velocities did not show a consistent trend in the angle of repose. To validate these observations, an Analysis of Variance (ANOVA) presented in Table 2 assessed the effects of three key parameters: layer thickness, rotational velocity, and translational velocity. In this table, DF represents degree of freedom, Adj SS represents adjusted sum of squares and adj MS represents adjusted mean of squares. The F-value is the ratio of the variance between the group means to the variance within the groups. The p-value, or probability value, is a measure used in statistical hypothesis testing to determine the significance of the observed results [37]. A significance level of 0.05 is used to determine the significance of the investigated factor. Layer thickness was identified as the most significant factor, accounting for 55.91% of the total variation, with a highly significant F-value of 110.55 ($p < 0.001$). Rotational velocity, however, had minimal impact,

contributing only 0.01% of the variation with a non-significant F-value of 0.03 (p = 0.868). Translational velocity similarly contributed 0.11% of the variation, supported by an insignificant F-value of 16.580 (p = 0.645). Additionally, the squared term of translational velocity showed a significant effect with an F-value of 46.46 (p = 0.000), accounting for 23.45% of the variation. The unexplained variation, indicated by the error term contributing 13.15%, highlights the complexity of the analysis. Overall, these findings emphasize the substantial influence of layer thickness on the dynamic angle of repose, consistent with existing literature [23], and underscore the minimal effect of rotational velocity in this context.

According to the results in the table, a response surface method equation was found to be as follows:

$$AoR = 30{,}1 + 0{,}051LT + 0{,}0118RV - 1{,}526TV - 0{,}000292LT * LT - 0{,}000102RV * RV + 0{,}02642TV * TV + 0{,}000201LT * RV + 0{,}00353LT * TV + 0{,}000103RV * TV \quad (5)$$

Table 2. Analysis of variance for dynamic angle of repose (AoR).

Source	DF	Contribution	Adj SS	Adj MS	F-Value	P-Value
Model	9	86,85%	206,005	22,889	19,08	0,000
Linear	3	56,03%	132,907	44,302	36,93	0,000
Layer Thickness (LY)	1	55,91%	132,612	132,612	110,55	0,000
Rotational Velocity (RV)	1	0,01%	0,034	0,034	0,03	0,868
Translational Velocity (TR)	1	0,11%	0,261	0,261	0,22	0,645
Square	3	23.97%	56.856	18.952	15.80	0.000
LT*LT	1	0.21%	0.492	0.492	0.41	0.527
RV*RV	1	0.22%	0.517	0.517	0.43	0.517
TV*TV	1	23.54%	55.847	55.847	46.56	0.000
2-Way Interaction	3	6.85%	16.242	5.414	4.51	0.011
LT*RV	1	0.51%	1.211	1.211	1.01	0.324
LT*TV	1	6.32%	14.989	14.989	12.50	0.002
RV*TV	1	0.02%	0.042	0.042	0.04	0.853
Error	26	13.15%	31.188	1.200		
Total	35	100.00%				

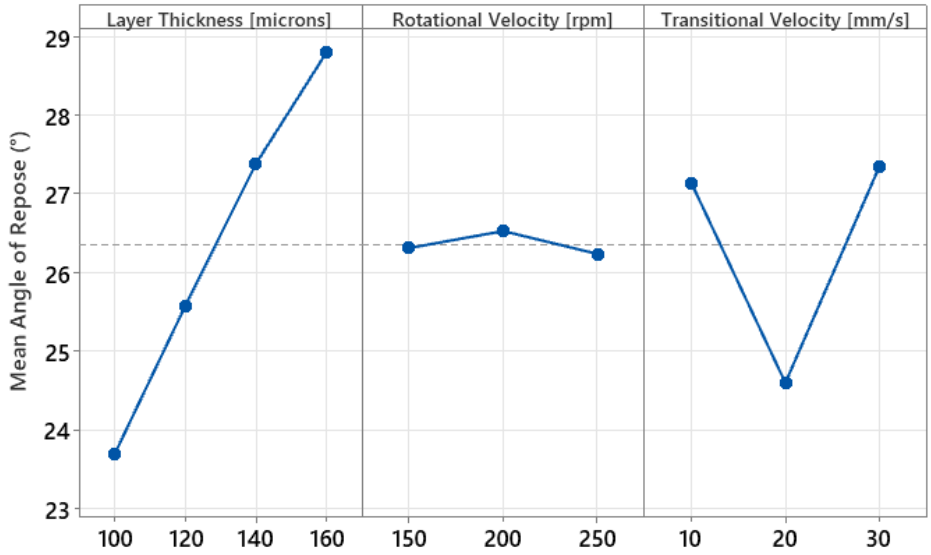

Figure 8. Parameters effect on volume packing fraction [%]

3.2. Bulk Density/Packing Fraction

Figure 8 provides insight into the main effects of volume packing fraction revealing that, under the investigated simulation parameters, increasing layer thickness and translational velocity lead to a significant decrease in volume packing fraction, while rotational velocity tends to increase it, consistent with findings by Haeri et al. [15] Zhang et al [30]. In their study, the translational velocities ranged from 40 mm/s to 160 mm/s and the volume packing fractions corresponding to these velocities ranged from 0.53 to 0.45, respectively. In the same study, when the effect of layer thickness on the volume packing fraction is considered, the volume packing fraction increases between 0.15 and 0.5, corresponding to a layer thickness of 50 microns and a layer thickness of 175 microns. However, the effect of rotational speed on volume packing fraction was found to be very small compared to other parameters. Fouda et al. also revealed similar findings. In their study, volume packing fractions corresponding to translational velocity speeds between 10 mm/s and 100 mm/s ranged between 47.5% and 25%. It is clearly seen that the increasing of translational velocity of roller reduces the packing volume fraction [18]. A similar situation was also found in this, the upper and lower values of volume packing fraction are determined to be 2800 kg/m³ and 2600 kg/m³, respectively. Table 3 presents the ANOVA results for volume packing fraction, offering further clarity on the influencing factors. Layer thickness emerges as a significant contributor, explaining 18.29% of the total variation with a highly significant F-Value of 124,28 ($p < 0.001$). Although rotational velocity demonstrates statistical significance, its impact is relatively modest, accounting for 3.69% of the variation (F-Value = 25.09, $p = 0.007$). In contrast, translational velocity emerges as the most influential factor, explaining a substantial 65.90% of the total variation, supported by a remarkably high F-Value of 447,86 ($p < 0.001$). Despite its lesser significance, rotational velocity still plays a discernible role. Overall, this analysis underscores the significant influence of layer thickness and translational velocity on volume packing fraction, highlighting the complexity of the system.

According to the results in the table, a response surface method equation was found to be as follows:

$$VPF = 70{,}03 + 0{,}0766RV - 0{,}5128TV + 0{,}000257LT * LT - 0{,}000082RV * RV + 0{,}00522TV * TV - 0{,}000181LT * RV + 0{,}001881LT * TV - 0{,}000589RV * TV \quad (6)$$

The literature commonly suggests that the dynamic angle of repose tends to increase with higher translational velocities. This trend typically indicates more challenging particle flow, leading to increased volume fraction and decreased production quality [38,39]. However, contrary to these expectations, this study did not yield clear statistical results regarding the dynamic angle of repose concerning the primary parameters. Notably, only the influence of layer thickness on the dynamic angle of repose was evident. As depicted in Figure 8, the effect of spreading parameters on volume packing fraction shows a very clear distribution, whereas no clear results were obtained for the effect on the dynamic angle of repose. Consequently, a direct correlation between increased layer thickness and the rise in the dynamic angle of repose is established. Nevertheless, despite this insight, a definitive relationship with volume packing fraction remains elusive.

In contrast to the statistical analysis regarding the dynamic angle of repose, notable findings emerge from the volume packing fraction analysis, demonstrating distinct results based on the parameters. The analysis reveals significant changes according to the three

primary parameters considered, suggesting meaningful relationships. As summarized in Figure 7, translational velocity notably influences volume packing fraction more than other factors. This observation aligns with findings from numerous studies in the literature (e.g., [4,21,40,41]), further emphasizing the substantial impact of translational velocity on volume packing fraction.

Table 3. Analysis of variance for volume packing fraction (VPF)

Source	DF	Contribution	Adj SS	Adj MS	F-Value	P-Value
Model	9	96.17%	110.268	122.520	72.63	0.000
Linear	3	87.88%	100,756	335.852	199.08	0.000
Layer Thickness (LY)	1	18.29%	20.967	209.669	124.28	0.000
Rotational Velocity (RV)	1	3.69%	4.233	42.333	25.09	0.000
Translational Velocity (TR)	1	65.90%	75.555	755.554	447.86	0.000
Square	3	2.53%	2.895	0.9651	5.72	0.004
LT*LT	1	0.33%	0.379	0.3792	2.25	0.146
RV*RV	1	0.29%	0.338	0.3379	2.00	0.169
TV*TV	1	1.90%	2.178	21.783	12.91	0.001
2-Way Interaction	3	5.77%	6.617	22.058	13.08	0.000
LT*RV	1	0.86%	0.983	0.9832	5.83	0.023
LT*TV	1	3.70%	4.246	42.457	25.17	0.000
RV*TV	1	1.21%	1.389	13.885	8.23	0.008
Error	26	3.83%	4.386	0.1687		
Total	35	100.00%				

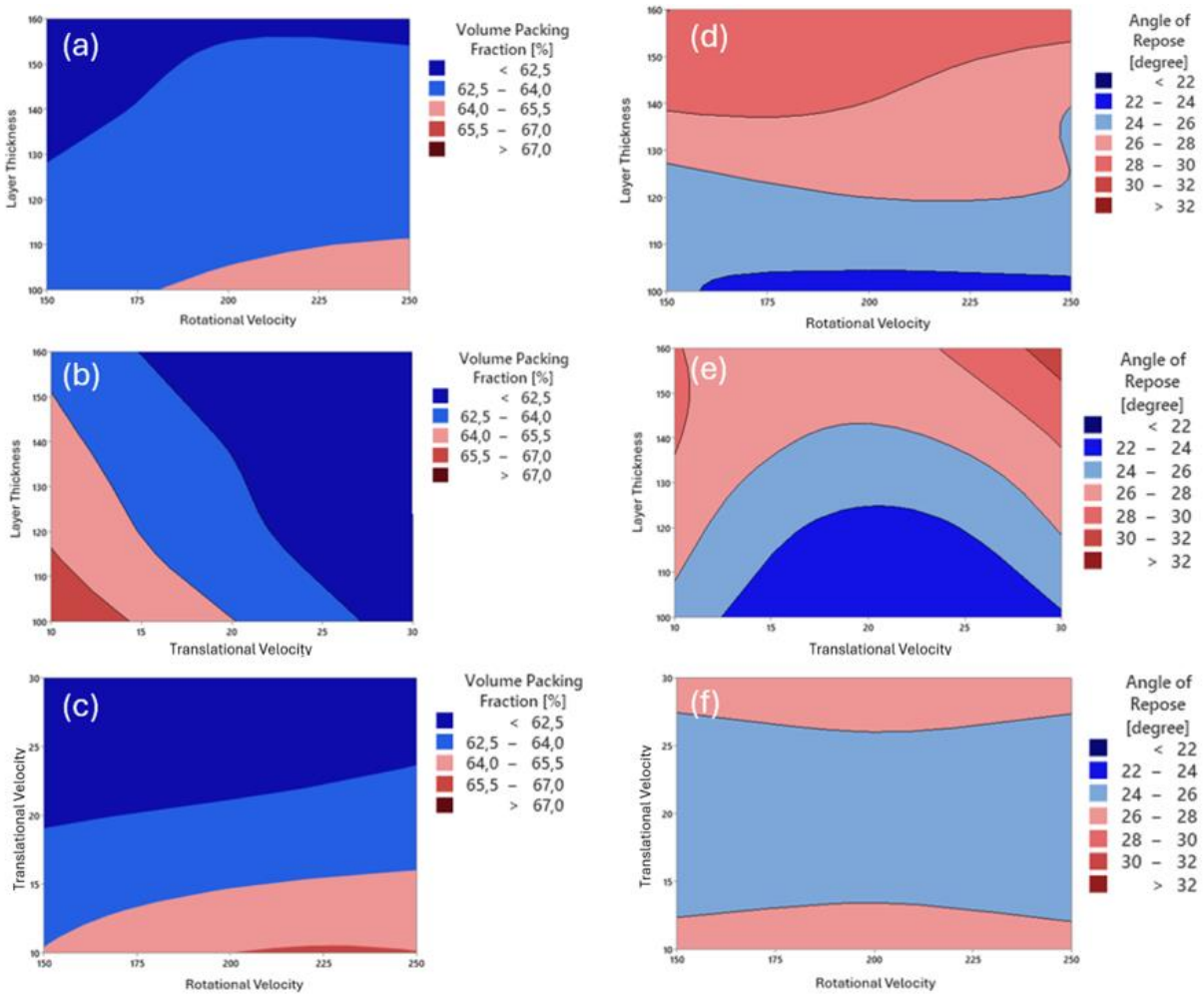

Figure 9. 2D contour plot for parameters effects on volume packing fraction a) Layer Thickness-Rotational Velocity, b) Layer Thickness -Translational Velocity, c) Translational Velocity -Rotational Velocity and Angle of Repose d) Layer Thickness – Rotational Velocity, e) Layer Thickness – Translational Velocity, f) Translational Velocity -Rotational Velocity

IV. CONCLUSIONS

This study numerically investigates the powder spreading behavior of Ti-6Al-4V alloy using the discrete element method, considering full factorial combinations of four levels of layer thickness, three levels of rotational velocity, and three levels of translational velocity. The simulation results were further evaluated using ANOVA. In conclusion, our investigation into the dynamic angle of repose and volume packing fraction reveals the intricate interplay between spreading parameters and material characteristics. Regarding the dynamic angle of repose, our findings align with existing literature, highlighting the pronounced influence of layer thickness and translational velocity. Notably, while rotational velocity showed statistical insignificance, layer thickness and translational velocity significantly affected the dynamic angle of repose, with translational velocity emerging as the most influential factor. However, contrary to expectations, no clear statistical results were obtained for the dynamic angle of repose concerning the main parameters, underscoring the complexity of the system. In contrast, our analysis of volume packing fraction reveals distinct results based on the parameters, with translational velocity exerting the most significant influence. Increasing layer thickness and translational velocity led to a notable decrease in volume packing fraction, while rotational velocity tended to increase it, consistent with previous research. These observations highlight the multifaceted nature of volume packing fraction determination, with translational velocity emerging as a key determinant. Overall, our study emphasizes the importance of considering multiple factors in understanding both the dynamic angle of repose and volume packing fraction.

It provides valuable insights into the complex dynamics of granular materials used in additive manufacturing. Further research into areas such as powder morphology variation and binder/powder interactions during spreading could enhance our understanding of particle behavior and inform the optimization of production processes. This study examined the spreading of the first layer in general. In fact, powder bed additive manufacturing methods involve the formation of multilayers and after each layer is spread, the binder is sprayed in binder jetting, while in applications such as electron beam melting and laser beam melting, each spread layer is molten. As a result of spraying the binder or melting the powder, the volume packing fraction of the layer changes and even the layer thickness decreases. Even such changes can be parameterized and added to the model. Improving the model used and studying this multilayer formation can lead to much more accurate results. In addition, due to the use of metal powders in this type of application, there is a magnetic attraction or repulsion between the powders. This may even occur between the powders and the binder. Such effects can also be added to the numerical model to produce better simulations that converge to reality.

REFERENCES

[1] Razavykia, A., Brusa, E., Delprete, C., and Yavari, R. (2020). An overview of additive manufacturing technologies-A review to technical synthesis in numerical study of selective laser melting. *Materials*. 13 (17), 1–22.

[2] Singh, R., Gupta, A., Tripathi, O., Srivastava, S., Singh, B., Awasthi, A., et al. (2019). Powder bed fusion process in additive manufacturing: An overview. *Materials Today: Proceedings*. 26 3058–3070.

[3] Dev Singh, D., Mahender, T., and Raji Reddy, A. (2021). Powder bed fusion process: A brief review. *Materials Today: Proceedings*. 46 350–355.

[4] Bai, Y., Wagner, G., and Williams, C.B. (2017). Effect of particle size distribution on powder packing and sintering in binder jetting additive manufacturing of metals. *Journal of Manufacturing Science and Engineering, Transactions of the ASME*. 139 (8), 1–6.

[5] Zhao, Y., Koizumi, Y., Aoyagi, K., Yamanaka, K., and Chiba, A. (2021). Thermal properties of powder beds in energy absorption and heat transfer during additive manufacturing with electron beam. *Powder Technology*. 381 44–54.

[6] Mostafaei, A., Elliott, A.M., Barnes, J.E., Li, F., Tan, W., Cramer, C.L., et al. (2021). Progress in Materials Science Binder jet 3D printing — Process parameters , materials , properties ,. *Progress in Materials Science*. 119 (June 2020), 100707.

[7] Onler, R., Koca, A.S., Kirim, B., and Soylemez, E. (2022). Multi-objective optimization of binder jet additive manufacturing of Co-Cr-Mo using machine learning. *International Journal of Advanced Manufacturing Technology*. 119 (1–2), 1091–1108.

[8] Gilabert, F.A., Roux, J.N., and Castellanos, A. (2007). Computer simulation of model cohesive powders: Influence of assembling procedure and contact laws on low consolidation states. *Physical Review E - Statistical, Nonlinear, and Soft Matter Physics*. 75 (1), 1–26.

[9] Maximenko, A.L., Olumor, I.D., Maidaniuk, A.P., and Olevsky, E.A. (2021). Modeling of effect of powder spreading on green body dimensional accuracy in additive manufacturing by binder jetting. *Powder Technology*. 385 60–68.

[10] Zhang, W., Mehta, A., Desai, P.S., and Fred Higgs, C. (2017). Machine learning enabled powder spreading process map for metal additive manufacturing (AM). *Solid Freeform Fabrication 2017: Proceedings of the 28th Annual International Solid Freeform Fabrication Symposium - An Additive Manufacturing Conference, SFF 2017*. 1235–1249.

[11] Miyanaji, H., Yang, L., and Momenzadeh, N. (2019). Effect of powder characteristics on parts fabricated via binder jetting process. *Rapid Prototyping Journal*. 25 (2),.

[12] Miyanaji, H., Orth, M., Akbar, J.M., and Yang, L. (2018). Process development for green part printing using binder jetting additive manufacturing. *Frontiers of Mechanical Engineering*. 13 (4), 504–512.

[13] Parteli, E.J.R. and Pöschel, T. (2016). Particle-based simulation of powder application in additive manufacturing. *Powder Technology*. 288 96–102.

[14] Mindt, H.W., Megahed, M., Lavery, N.P., Holmes, M.A., and Brown, S.G.R. (2015). Powder Bed Layer Characteristics : The Overseen First-Order Process Input. *Metallurgical and Materials Transactions A*.

[15] Haeri, S. (2017). Optimisation of blade type spreaders for powder bed preparation in Additive Manufacturing using DEM simulations. *Powder Technology*. 321 94–104.

[16] Meier, C., Weissbach, R., Weinberg, J., Wall, W.A., and Hart, A.J. (2019). Critical influences of particle size and adhesion on the powder layer uniformity in metal additive manufacturing. *Journal of Materials Processing Technology*. 266 (August 2018), 484–501.

[17] Nan, W., Pasha, M., Bonakdar, T., Lopez, A., Zafar, U., Nadimi, S., et al. (2018). Jamming during particle spreading in additive manufacturing. *Powder Technology*. 338 253–262.

[18] Fouda, Y.M. and Bayly, A.E. (2020). A DEM study of powder spreading in additive layer manufacturing. *Granular Matter*. 22 (1).

[19] Han, Q., Gu, H., and Setchi, R. (2019). Discrete element simulation of powder layer thickness in laser additive manufacturing. *Powder Technology*. 352 91–102.

[20] Phua, A., Cook, P.S., Davies, C.H.J., and Delaney, G.W. (2022). Powder spreading over realistic laser melted surfaces in metal additive manufacturing. *Additive Manufacturing Letters*. 3 (February), 100039.

[21] Lee, Y., Gurnon, A.K., Bodner, D., and Simunovic, S. (2020). Effect of Particle Spreading Dynamics on Powder Bed Quality in Metal Additive Manufacturing. *Integrating Materials and Manufacturing Innovation*. 9 (4), 410–422.

[22] Chen, H., Chen, Y., Liu, Y., Wei, Q., Shi, Y., and Yan, W. (2020). Packing quality of powder layer during counter-rolling-type powder spreading process in additive manufacturing. *International Journal of Machine Tools and Manufacture*. 153.

[23] Lampitella, V., Trofa, M., Astarita, A., and D'Avino, G. (2021). Discrete element method analysis of the spreading mechanism and its influence on powder bed characteristics in additive manufacturing. *Micromachines*. 12 (4), 392.

[24] Burman, B.C., Cundall, P.A., and Strack, O.D.L. (1980). A discrete numerical model for granular assemblies. *Geotechnique*. 30 (3), 331–336.

[25] Tsuji, Y., Tanaka, T., and Ishida, T. (1992). Lagrangian numerical simulation of plug flow of cohesionless particles in a horizontal pipe. *Powder Technology*. 71 (3), 239–250.

[26] Di Renzo, A. and Di Maio, F.P. (2004). Comparison of contact-force models for the simulation of collisions in DEM-based granular flow codes. *Chemical Engineering Science*. 59 (3), 525–541.

[27] Arratia, P.E., Duong, N. hang, Muzzio, F.J., Godbole, P., and Reynolds, S. (2006). A study of the mixing and segregation mechanisms in the Bohle Tote blender via DEM simulations. *Powder Technology*. 164 (1), 50–57.

[28] Hassanpour, A., Tan, H., Bayly, A., Gopalkrishnan, P., Ng, B., and Ghadiri, M. (2011). Analysis of particle motion in a paddle mixer using Discrete Element Method (DEM). *Powder Technology*. 206 (1–2), 189–194.

[29] Gong, H., Rafi, K., Gu, H., Janaki Ram, G.D., Starr, T., and Stucker, B. (2015). Influence of defects on mechanical properties of Ti-6Al-4V components produced by selective laser melting and electron beam melting. *Materials and Design*. 86 545–554.

[30] Zhang, J., Tan, Y., Bao, T., Xu, Y., Xiao, X., and Jiang, S. (2020). Discrete element simulation of the effect of roller-spreading parameters on powder-bed density in additive manufacturing. *Materials*. 13 (10).

[31] Körner, C., Attar, E., and Heinl, P. (2011). Mesoscopic simulation of selective beam melting processes. *Journal of Materials Processing Technology*. 211 (6), 978–987.

[32] Körner, C. and Körner, C. (2016). Additive manufacturing of metallic components by selective electron beam melting — a review 6608 (May).

[33] Ahmed, M., Pasha, M., Nan, W., and Ghadiri, M. (2020) A simple method for assessing powder spreadability for additive manufacturing. *Powder Technology*. 367 671–679.

[34] Chen, H., Wei, Q., Wen, S., Li, Z., and Shi, Y. (2017). Flow behavior of powder particles in layering process of selective laser melting: Numerical modeling and experimental verification based on discrete element method. *International Journal of Machine Tools and Manufacture*. 123 (August), 146–159.

[35] Chen, H., Wei, Q., Zhang, Y., Chen, F., Shi, Y., and Yan, W. (2019). Powder-spreading mechanisms in powder-bed-based additive manufacturing: Experiments and computational modeling. *Acta Materialia*. 179 158–171.

[36] Sklar, J. (2013). Minitab® Manual.

[37] W, Svante., S, Lars. (1989). Analysis of Variance (ANOVA). *Chemometrics and Intelligent Laboratory*. 6(4), 259-272.

[38] Vaezi, M. and Chua, C.K. (2011). Effects of layer thickness and binder saturation level parameters on 3D printing process. *International Journal of Advanced Manufacturing Technology*. 53 (1–4), 275–284.

[39] Cao, S., Qiu, Y., Wei, X.F., and Zhang, H.H. (2015). Experimental and theoretical investigation on ultra-thin powder layering in three dimensional printing (3DP) by a novel double-smoothing mechanism. *Journal of Materials Processing Technology*. 220 231–242.

[40] Wu, S., Lei, Z., Jiang, M., Liang, J., Li, B., and Chen, Y. (2022). Experimental investigation and discrete element modeling for particle-scale powder spreading dynamics in powder-bed-fusion-based additive manufacturing. *Powder Technology*. 117390.

[41] Chen, H., Cheng, T., Li, Z., Wei, Q., and Yan, W. (2022). Is high-speed powder spreading really unfavourable for the part quality of laser powder bed fusion additive manufacturing? *Acta Materialia*. 231 117901.